A dansyl-derivatized phytic acid analogue as a fluorescent substrate for phytases: experimental and computational approach

Christophe Dussouy, Eric Dubreucq, Patrick Chemardin, Véronique Perrier, Josiane Abadie, Hervé Quiquampoix, Claude Plassard, Jean-Bernard Behr

Version of Record: https://www.sciencedirect.com/science/article/pii/S0045206821001875
Manuscript_0ca243658fb3ccaa78d771fd38ccf968

A dansyl-derivatized phytic acid analogue as a fluorescent substrate for phytases: experimental and computational approach

Christophe Dussouy[1], Eric Dubreucq[2], Patrick Chemardin[3], Véronique Perrier[2], Josiane Abadie[4], Hervé Quiquampoix[4], Claude Plassard[4]* and Jean-Bernard Behr[1]*

[1]Université de Reims Champagne Ardenne, CNRS, ICMR UMR 7312, 51097 Reims, France.
[2]IATE, Université Montpellier, INRAE, Institut Agro, Montpellier, France.
[3]SPO, Université Montpellier, INRAE, Institut Agro, Montpellier, France.
[4]Eco&Sols, Université Montpellier, CIRAD, INRAE, Institut Agro, IRD, Montpellier, France.

Fax: +33 326 91 31 66 ; E-mail : jb.behr@univ-reims.fr

Graphical abstract :

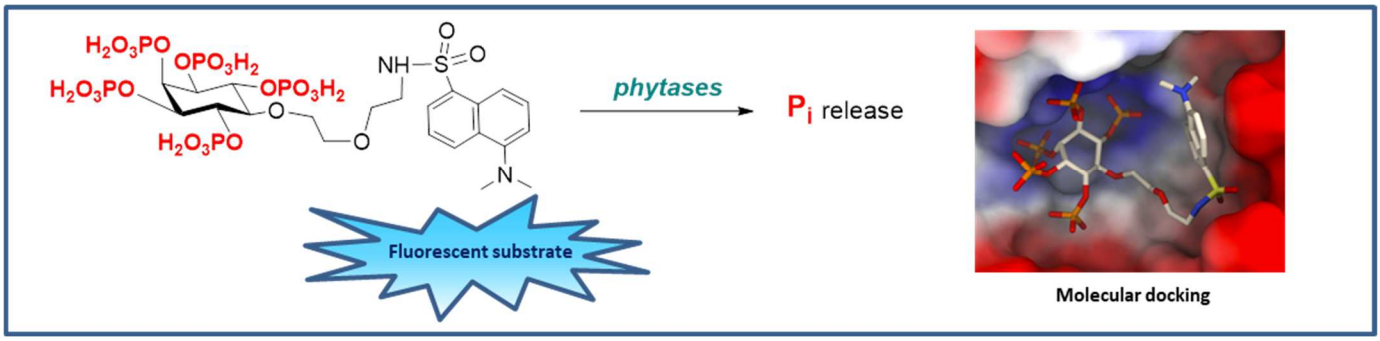

Abstract

A new *myo*-inositol pentakisphosphate was synthesized, which featured a dansyl group at position C-5. The fluorescent tag was removed from the inositol by a 6-atom spacer to prevent detrimental steric interactions in the catalytic site of phytases. The PEG linker was used in order to enhance hydrophilicity and biocompatibility of the new artificial substrate. Computational studies showed a favorable positioning in the catalytic site of phytases. Enzymatic assays demonstrated that the tethered *myo*-inositol was processed by two recombinant phytases Phy-A and Phy-C, classified

respectively as acid and alkaline phytases, with similar rates of phosphate release compared to their natural substrate.

Keywords: phosphate, soil, fertilizer, inositol-phosphates, phytases, kinetics, artificial substrate

1. Introduction

Inositol-phosphates are phosphate esters of cyclohexanhexol, which are involved in a wide range of biological processes [1]. Originally found in plants [2], this family of inositol compounds was also identified later in humans, where they play key roles in the regulation of ion uptake [3]. In particular, inositol 1,4,5-triphosphate promotes the release of Ca^{2+}, a biological mediator linked to cell proliferation, muscle contraction, apoptosis or gene transcription [4] Among the nine possible stereoisomers of cyclohexanhexol, *myo*-inositol **1** is the most relevant, although *scyllo*-, *chiro*- and *neo*-inositol have also been isolated from animal tissues and are present in soils [5] (Figure 1). *Myo*-inositol hexakisphosphate, or phytic acid **2** (abbreviated as InsP_6 according to IUPAC recommendations) and its salts (named phytates) is sequentially biodegraded to afford partially phosphorylated inositol penta- (InsP_5), tetra- (InsP_4), tri- (InsP_3), bis- (InsP_2) or mono-phosphates (InsP_1). Phytic acid is the major storage form of phosphorous in plant seeds and makes inputs to soil through two main ways [6a]. The first one is the fall of seeds to the ground and the second one is the use of manures produced by monogastric animals as they are not able to degrade phytate from seeds. Taken as a whole, phytic acid might comprise up to 58% of soil organic phosphorus [6b]. However, due to the lack of phytate membrane transporters in roots [6a], plants cannot absorb directly phytate. To be processed by plants, orthophosphate must be released from its organic source by specific enzymes known as phytases. However, most of plant species are not able to secrete phytases in their root environment [6c]. In contrast, microorganisms produce extracellular phytases responsible for phytate hydrolysis, which can represent a crucial step in the P-cycle. So far, four classes of phytases have been identified on phylogenetic kinship [7]: purple acid phosphatase phytase (PAPhytase), histidine acid phytase (HAP), cysteine phosphatase-like phytase (CP-phytase), and ß-propeller phytase (BPP) [8]. Phytases are also characterized according to their mechanism of action as 3-phytases (EC 3.1.3.8), which initiate hydrolysis preferentially at the C-3 position, and 6-phytases (EC 3.1.3.26), which process at C-6. Although a great deal is known about the biological relevance of microbial phytases in soil, gaps still remain in the understanding of their accurate mode of action. This is due to the difficulty to follow phytate hydrolysis in soil because the released orthophosphate (i) will be trapped by adsorption on soil mineral surfaces such as clays or

oxides and oxyhydroxides of Fe and Al and (ii) will be difficult to distinguish from endogenous orthophosphate. Therefore, it would be more efficient to extract and to identify by HPLC the various phosphorylated inositols potentially generated by the microbial phytases following phytate addition to the soil. Hence, to gain knowledge in the localization, the role and the mode of action of phytases, more easily detectable substrates are needed. A first artificial phytate analogue has been prepared by Berry *et al* in 2005 [9]. The benzoylated analogue **3** (Fig. 1) was used to measure phytase activity in soils through the identification of hydrolysis products (Ins$P_{6\text{-n}}$) by HPLC. However, relatively high concentrations of substrate were needed in biological assays due to the low absorbance of the benzoyl chromophore. Another artificial phytate from commercial sources was used more recently to the same purpose, but no information was available on its synthetic preparation [10a,b].

In this investigation we report the development of the new fluorogenic phytic acid analogue **4a** (Fig. 1) and the validation of its value as an efficient substrate for two recombinant phytases that are (i) the HAP phytase (Phy-A) from *Aspergillus niger* (EC 3.1.3.8) [11] and (ii) the BPP phytase (Phy-C) from *Bacillus subtilis* (EC 3.1.3.8) [12]. Although both enzymes are 3-phytases, their end products are different with InsP*1* for PhyA and InsP*3* for PhyC. In addition, PhyC requires calcium for its activity. Our final goal is to use **4a** as a chemical probe for assaying phytase activity in soils. For this reason an efficient synthetic route enabling the production of preparative amount of **4a** is needed [10b].

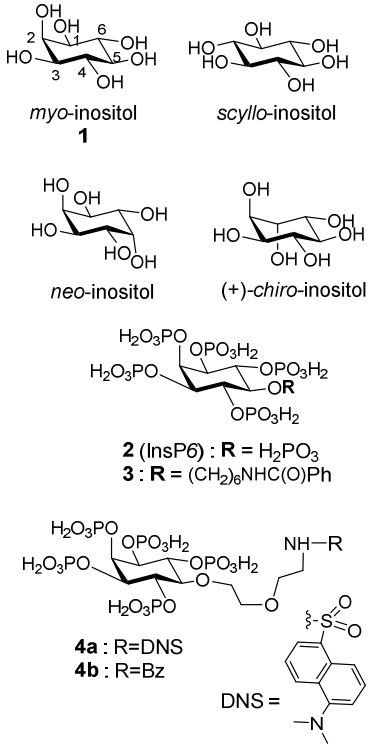

Fig. 1. Structures of key compounds.

2. Results and Discussion

2.1. Substrate design

The preparation of a suitable substrate for 3- or 6- phytases raised several issues. The choice of the tethered position was crucial to allow a possible action of both classes of enzymes. Thus, we intended to install the chromophoric substituent at the non-reactive position C-5. Furthermore, synthetic modifications at this position would minimize stereochemical issues, keeping the intermediates and the final compound as *meso* forms. According to structure **3** (Fig. 1), moving the chromophoric species away from the inositol by a spacer allows to retain affinity for the active site of phytase. The introduction of a PEG linker would also enhance hydrophilicity and biocompatibility of the artificial substrate [13]. Finally, the introduction of a fluorogenic probe, the detection of which is much more sensitive than UV-absorbance, would address the sensitivity issues. The dansyl fluorescent label seemed particularly attractive as it has been used with success for biological purposes, in the synthesis of fluorescently labeled substrate analogues for chitin synthase for instance [14]. The choice of the dansyl group preferably to BODIPY dyes, cyanines, coumarins or other fluorogenic labeling strategies for biological purposes was its ease of handling, its stability in biological medium, its stability to various chemical transformations, its commercial availability and low price and its compatibility with some enzymatic targets.

The compatibility of the dansyl derivative with the active site of phytases was confirmed by molecular docking calculations performed with structures of the Phy-A and Phy-C phytases crystallized in complex with phytate analogue *myo*-inositol-1,2,3,4,5,6-hexakis sulfate and, for Phy-C, Ca^{2+} [15,16] (PDB entries 3K4Q and 3AMR, respectively). As shown on Figure 2, the presence of the linked dansyl group did not seem to interfere with the binding of the phytate moiety at the same location as for the natural phytate and allowed a similar positioning of phosphate groups in the catalytic cavity.

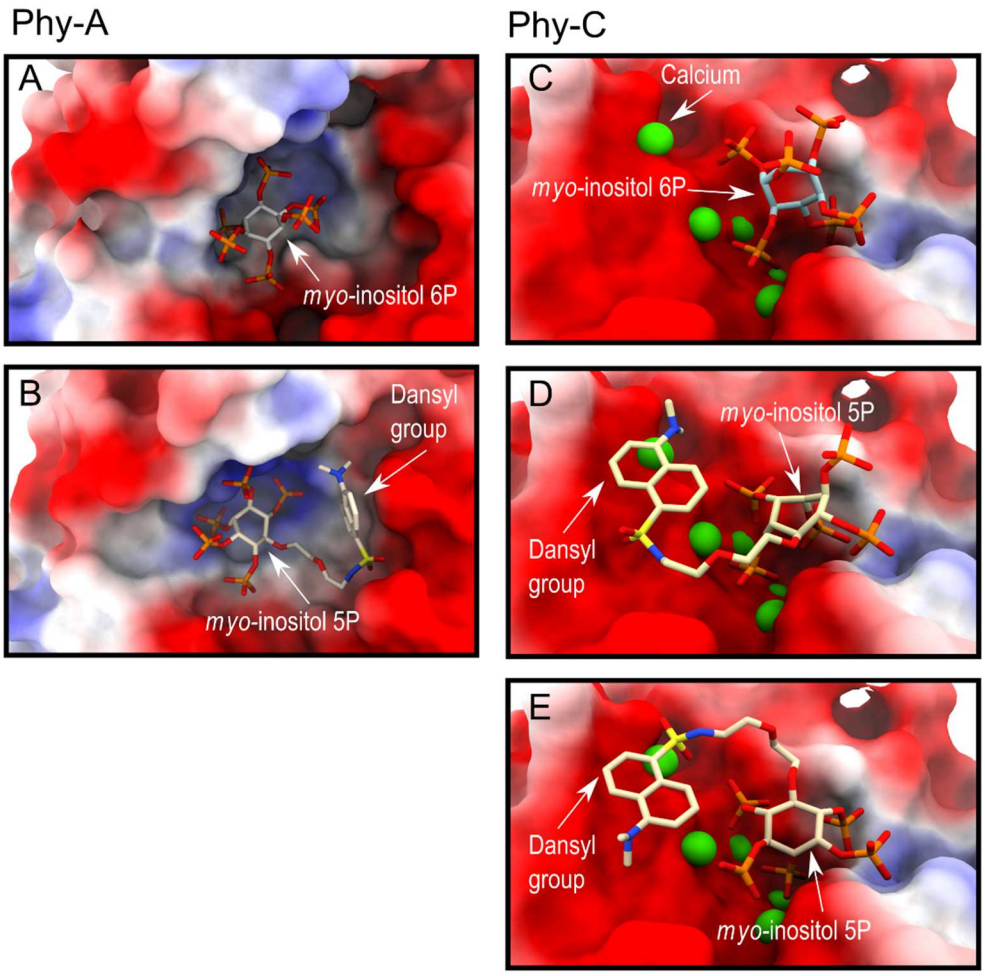

Fig. 2. Molecular modelling of the positioning of the inositol phosphate moiety in the catalytic site of Phy-A (A, B) or Phy-C (C, D, E) when *myo*-inositol 6P (A, C) or *myo*-inositol 5P with a fluorogenic group (dansyl group) (B, D, E) is supplied. Figures show the poses with highest docking score after energy minimization of the structure in an explicit water box. Docking scores by Autodock Vina were -6.3 kcal/mol (A), -7.3 (B), -5.2 (C), -6.0 (D) and -6.0 (E). For both enzymes, the red and blue colors indicate negative and positive electrostatic potential, respectively. In Phy-C, calcium ions are in green.

2.2. Chemistry

Since our final goal is to profile phytase activity in environments, preparative amounts of artificial substrate are needed. For this reason we wished to come up with a reliable synthetic route to **4a** (Fig. 1), which could be applicable on a large scale.

A three-stage method of *myo*-inositol protection/deprotection was envisioned to keep hydroxyl at position C-5 free for further functionalization. For this, positions 1,3 and 5 were simultaneously protected by reaction with triethyl orthoformate, according to a known reaction (scheme 1) [17]. Benzylation of the remaining free hydroxyls was then performed under standard conditions to

afford fully protected inositol **6**. Regioselective reduction of the orthoformate with diisobutylaluminium hydride (solution in hexanes) yielded compound **7**, which featured an unprotected OH group at C-5 as expected. This transformation was highly efficient and afforded quantitatively **7** after 2 h at room temperature in the presence of 2.5 equivalents of hydride. During this latter stage, when a solution of DIBAL-H *in THF* was used instead of the solution in hexanes, only poor conversion was reached under the same experimental conditions. The choice of the source of hydride was thus crucial to succeed in this transformation.

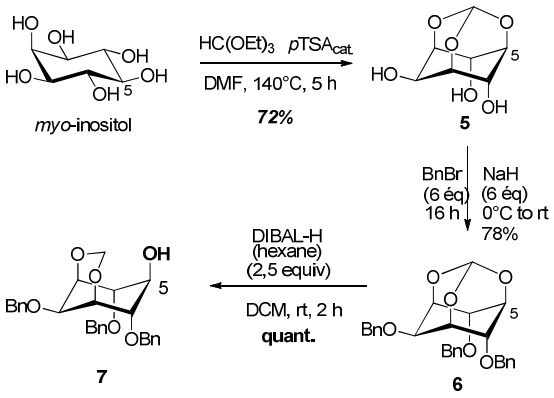

Scheme 1. Synthesis of intermediate **7**.

The attachment of an ethyleneglycol derived linker to inositol **7** was anticipated by simple nucleophilc substitution of an activated form (mesylate) of the linker with C5-OH. The linker should also feature an amino function at the opposite end to tether the chromophore. To this aim we prepared mesylates **9** and **11** from commercial 2-(2-aminoethoxy)ethanol **8** and 2-(2-chloroethoxy)ethanol **9** respectively. Standard protection of amine **8** with di-tert-butyl dicarbonate followed by mesylation with methanesulfonyl chloride afforded **9** in 90% overall yield (Scheme 2). Chloride **10** was treated with NaN_3 for 2 days in refluxing water and the resulting hydroxyl-azide was mesylated as above to give **11** (72%, two steps) [18]. In the next step, whereas azide **11** reacted efficiently with inositol **7** in the presence of NaH to afford **12** (90% yield), the same reaction with protected amine **9** proved unsuccessful. Instead, intramolecular reaction was kinetically favored and only morpholine **13** was isolated along with unreacted inositol.

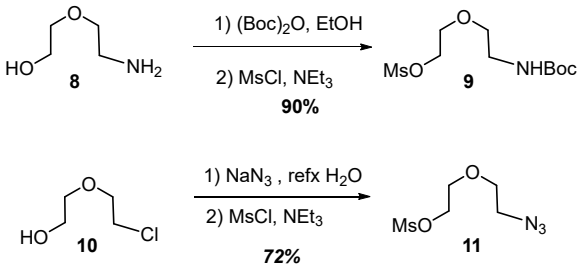

Scheme 2. Syntheses of linkers.

In order to make the synthetic route versatile and applicable in the future to a range of fluorogenic species we intended to attach the chromophoric structure at the later steps of the synthesis, that is on the fully deprotected inositol-amine **15** (Scheme 3). Thus, azide **12** was treated with boron trichloride at 0 °C to remove both the acetal and the benzyl groups in a very smooth manner affording azide-pentol **14** in good yields. Reduction of **14** under Staudinger's conditions afforded amine **15** quatitatively. However, reaction of dansyl chloride with unprotected **15** proved difficult and yields did not exceed 60%. A more reliable sequence was obtained by switching the steps and by introducing the dansyl group before deprotection. Thus, reduction of azide was effected first on compound **12** to afford quantitatively amine **17**, which was reacted without further purification with DNS-Cl to give the corresponding tethered inositol **18** in 81% yield. Final deprotection with BCl_3 proved as efficient as above affording **16** in 98% yield. In parallel, amine **17** was functionalized likewise with a benzoyl group affording inositol **19** and its deprotected analogue **20**, showing the versatility of the synthetic route.

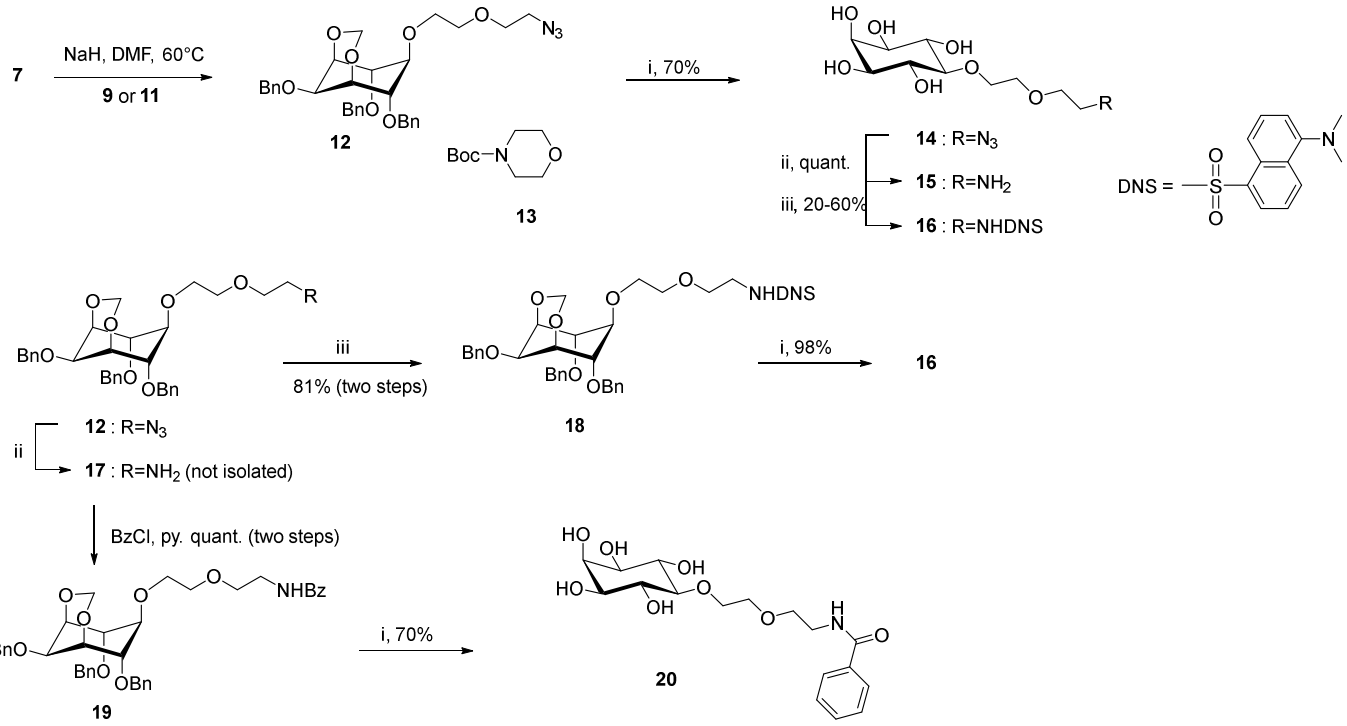

Scheme 3. Synthesis of tethered *myo*-inositols, experimental conditions : i : BCl_3, 0 °C, then MeOH; ii : PPh_3, DMF/H_2O, 50 °C, 24 h; iii : DNS-Cl, NEt_3, DMF, rt.

The phosphorylation sequence of inositols is a standard procedure requiring an excess (usually 2 equivalents per hydroxyl) of *O*-dibenzyl or *O*-ortho-xylylene-phosphoramidite followed by

oxidation to the expected phosphate with mCPBA [19]. The presence of an acid activator is usually necessary to assume complete and rapid conversion. Tetrazole and derivatives thereof are commonly used, but pyridinium trifluoroacetate (PyTFA) showed also good results. Initial phosphorylation attempts of dansyl-inositol **16** were conducted under various conditions, using either dibenzyl *N*,*N*-diisopropylphosphoramidite or *o*-xylylene *N,N*-diethylphosphoramidite as the phosphorylating agent and PyTFA or 5-phenyltetrazole as the activator (Scheme 4). Though complete conversion of the starting material occurred, the expected pentaphosphate **21** was isolated in only poor yields. Conversely, a control reaction with benzoylated inositol **20** proved successful, affording **22** in 90% yield. This result calls into questions the compatibility of the dansyl group with the reaction conditions. Particularly, oxidation with mCPBA, although it is conducted at low temperature, could affect the sulfonamide group. To control the stability of dansyl in the presence of mCPBA, a solution of inositol **16** and the peracid was stirred for 1h30 in dichloromethane. NMR analysis of the crude mixture revealed the conversion of 50% of the starting material into degradation products, confirming the incompatibility of the DNS moiety with mCPBA. Iodine was also checked as the oxidant in a further assay, with no improvement in the yields. Finally, the use of oxygen peroxide allowed selective oxidation of the phosphoramidite function without degradation of the chromophore. However, yields of the expected phosphate **21** did not exceed 35%. Indeed, a side product rising from additional phosphorylation at nitrogen could also be isolated [20]. This side reaction could be minimized by simply lowering the amount of phosphoramidite from 10 equivalents to 6.6 affording **21** in 72% yield. During the final debenzylation step, the amount of Pd-C had to be carefuly checked. Indeed, uncoupling of DNS occurred when performing the first assays of hydrogenation in the presence of a 1.4-fold amount of Pd-C *vs* benzyl-protected substrate **21**, affording the expected pentaphosphate **4a** in unsatisfactory 20% yield. Optimization of the reaction conditions (amount of catalyst, time of reaction, method of purification of final compound) permitted to improve the isolated yields up to 56%. A first preparative synthesis of DNS-phytate **4a** was conducted and permitted to isolate 0.8 g of final compound by debenzylation of 3.55 g of protected inositol **21**. Its use as substrate for various phytases was examined further to evaluate its potential as a chemical tool for biological purposes.

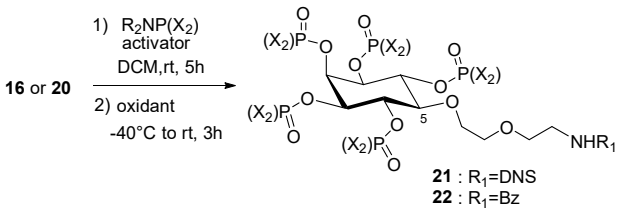

substrate	$R_2NP(X_2)$	activator	oxidant	product (yield)
16	$iPr_2NP(OBn)_2$	PyTFA[a]	*m*CPBA	**21** (20%)
16	$Et_2NP(OXyl)_2$	PyTFA	*m*CPBA	**21** (15%)
16	$iPr_2NP(OBn)_2$	PTA[b]	*m*CPBA	**21** (25%)
20	$iPr_2NP(OBn)_2$	PTA	*m*CPBA	**22** (90%)
16	$iPr_2NP(OBn)_2$[c]	PTA	H_2O_2	**21** (35%)[d]
16	$iPr_2NP(OBn)_2$[e]	PTA	H_2O_2	**21** (72%)

[a] Pyridinium trifluoroacetate; [b] 5-phenyltetrazole; [c] 10 equiv.; [d] The N-phosphorylated analogue of **19** was also formed; [e] 6.6 equiv.

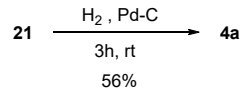

Scheme 4. phosphorylation/hydrogenolysis steps.

*2.3. Use of fluorescent substrate **4a** by phytases*

A sample of compound **4a** might be stored at -20°C without any degradation. Only 5% autogenic release of phosphate was measured with a sample that was stored at room temperature for several months. Further control was performed by NMR analysis in water (D_2O), which proved its complete stability for at least 48h in this solvent (pH 1), without any degradation. The potential of fluorescent *myo*-inositol phosphate **4a** to act as a substrate for phytases was then verified using two recombinant enzymes produced by gene overexpression in the yeast *Komagataella* (*Pichia) pastoris*: one fungal histidine acid phytase from *Aspergillus niger* (Phy-A) and one bacterial ß-propeller phytase from *Bacillus subtilis* (Phy-C). Both enzymes were assayed with their natural substrate *myo*-inositol hexakisphosphate and with our new fluorescent 5-(dansylaminoethoxy)ethyl-*myo*-inositol-pentaphosphate. Reaction rates were estimated by measurement of Pi release using the Malachite green method (see experimental part).

In the reaction conditions tested, using *myo*-inositol hexakisphosphate (sodium salt), Phy-A proved significantly more active than Phy-C (0.65 µmol.s^{-1}.mg^{-1} protein *vs* 0.10 µmol.s^{-1}.mg^{-1} protein) (Fig. 3). Despite belonging to two very different phytase families, both enzymes released free Pi from our artificial substrate **4a** at the same rate as for the natural substrate (0.60 µmol.s^{-1}.mg^{-1} protein and 0.13 µmol.s^{-1}.mg^{-1} protein, respectively) (Fig. 3). The calculated conversion after 5 minutes (end-point) are for PhyA, 37,47±1,8 % with Na-phytate and 37,41±2,9 % with 4a (n=3), for PhyC, 21,6 ±1,29 % with Na-phytate and 23,47±3,7 % with 4a (n=3). Taken together, these results demonstrated that **4a** is a valuable phytase substrate and that the addition of the fluorogenic group did not alter recognition of the phytate moiety of the substrate by either enzyme.

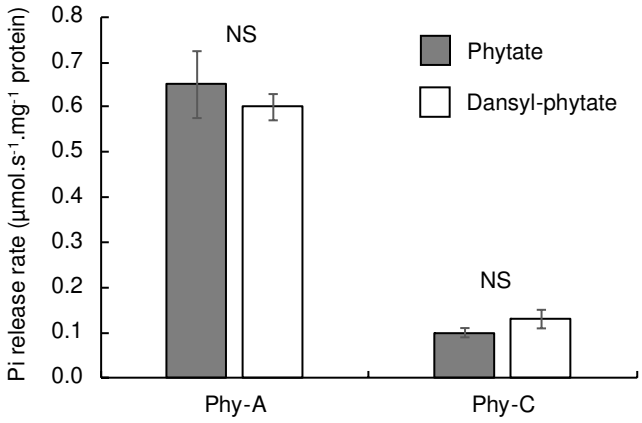

Fig. 3. Rates of inorganic Pi release, expressed in µmol.s^{-1}.mg^{-1} protein, by Phy-A and Phy-C incubated with *myo*-inositol-hexaphosphate (Phytate) or 5-(dansylaminoethoxy)ethyl-*myo*-inositol-pentaphosphate (Dansyl-phytate) supplied as their sodium salts. Note that calcium, as a required co-factor, was added to the substrate for incubating Phy-C. Values are means with standard deviation between brackets (n=3). For each enzyme, no significant differences were found between means measured with either substrate (NS, *Student's t-test*).

3. Conclusions

In conclusion, we prepared a chromogenic analogue of *myo*-inositol hexaphosphate, which features a dansyl group at position C-5. Compound **4a** might be used as a non-natural substrate for phytases in order to follow enzyme kinetics more conveniently. Preliminary docking experiments conducted with structures of Phy-A and Phy-C (PDB entries 3K4Q and 3AMR) confirmed the compatibility of the dansyl derivative with the active site of phytases. The presence of the tethered dansyl group might not impede the binding of the phytate moiety and allows a similar positioning of phosphate groups into the catalytic cavity. Two enzymes, (Phy-A from *Aspergillus niger* and Phy-C from *Bacillus subtilis*) were shown to operate experimentally with the chromogenic substrate, at rates which were comparable to those observed for the natural substrate (sodium phytate). Hence, the new substrate **4a** will be useful to assess the actual phytate hydrolysis in soil by microbial extracellular phytases.

4. Experimental section

4.1. Chemistry

4.1.1 Reagents and methods

Reactants and reagents were purchased from Aldrich and Sigma and were used without further purification. Silica gel F254 (0.2 mm) was used for TLC plates, detection being carried out by spraying with an alcoholic solution of phosphomolybdic acid, followed by heating. Flash column chromatography was performed over silica gel M 9385 (40-63 μm) Kieselgel 60. NMR spectra were recorded on Bruker AC 250 (250 MHz for ^{1}H, 62.5 MHz for ^{13}C) or 500 (500 MHz for ^{1}H, 125 MHz for ^{13}C) spectrometers. Chemical shifts are expressed in parts per million (ppm) and were calibrated to the residual solvent peak. Coupling constants are in Hz and splitting pattern abbreviations are: br, broad; s, singlet; d, doublet; t, triplet; m, multiplet. High Resolution Mass Spectra (HRMS) were performed on Q-TOF Micro micromass positive ESI (CV = 30 V).

4.1.2 Syntheses

4.1.2.1. 5-*O*-[2-(2-Azidoethoxy)ethyl)-2,3,4-tri-*O*-benzyl-1,3-*O*-methylidene-*myo*-inositol (12)

To a solution of inositol **7** (500 mg, 1.08 mmol) in DMF (10 ml) at 0°C under an atmosphere of argon, was added NaH (60% dispersion in mineral oil, 129.6 mg, 3.24 mmol, 3 eq). The mixture was stirred for 20 min and a solution of 2-(2-Azidoethoxy)ethyl) methanesulfonate **11** (452 mg, 2.16 mmol, 2 eq) in DMF (10 ml) was added slowly. The mixture was stirred for 30 min at 0°C and then heated to 80°C. After 18 h the reaction mixture was cooled to RT, poured into ice and extracted with 3x50 ml of Et_2O. The organic layers were washed with water (50 ml) and $NaHCO_3$ (2x50 ml). The combined organic phases were dried ($MgSO_4$), filtered, and concentrated under reduced pressure. The residue was purified by chromatography on silica gel in Tol/EA 95/5 to 9/1 to give **12** (560 mg ; 0.97 mmol ; 90%) as a colorless oil. R_f = 0.49 with Tol/EA 8/2. ^{1}H NMR (500 MHz, $CDCl_3$) δ 7.47 – 7.27 (m, 15H, C<u>*H*</u> (Bn)), 5.18 (d, J_{HaHb} = 5.6 Hz, 1H, Ha), 4.85 (d, J_{HbHa} = 5.6 Hz, 1H, Hb), 4.69 (d, J = 11.7 Hz, 2H, C<u>*H*</u>$_2$ (Bn)), 4.67 (s, 2H, C<u>*H*</u>$_2$ (Bn)), 4.64 (d, J = 11.7 Hz, 2H, C<u>*H*</u>$_2$ (Bn)), 4.27 (d, $J_{H1H2} = J_{H3H2}$ = 1.1 Hz, 2H, H_1, H_3), 3.94 (d, $J_{H4H5} = J_{H6H5}$ = 6.1 Hz, 2H, H_4, H_6), 3.84 – 3.80 (m, 3H, H_2, $H_{A'}$), 3.65 – 3.59 (m, 4H, $H_{B'}$, $H_{C'}$), 3.54 (t, $J_{H5H4} = J_{H5H6}$ = 6.1 Hz, 1H, H_5), 3.32 (t, $J_{HD'HC'}$ = 5.1 Hz, 2H, $H_{D'}$). ^{13}C NMR (126 MHz, $CDCl_3$) δ 137.88 (2<u>*C*</u>, Bn), 137.70 (<u>*C*</u>, Bn), 128.56, 128.51, 127.95, 127.93, 127.90, 127.86 (15<u>*C*</u>H, Bn), 85.61 (<u>*C*</u>H_2, <u>*C*</u>HaHb), 82.29 (2<u>*C*</u>H, C_4, C_6), 81.80 (<u>*C*</u>H, C_5), 72.24 (2<u>*C*</u>H, C_1, C_3), 71.90 (2x<u>*C*</u>H_2, Bn), 71.31 (<u>*C*</u>H_2, $C_{A'}$),

71.07 (<u>C</u>H$_2$, Bn), 70.86 (<u>C</u>H$_2$, C$_{B'}$), 70.24 (<u>C</u>H, C$_2$), 70.01 (<u>C</u>H$_2$, C$_{C'}$), 50.75 (<u>C</u>H$_2$, C$_{D'}$). HRMS *m/z* [M + Na]$^+$ calculated for $C_{32}H_{37}N_3O_7Na$ 598.2534, found 598.2529.

4.1.2.2. 2,3,4-tri-*O*-Benzyl-5-*O*-[2-(2-dansylaminoethoxy)ethyl)-1,3-*O*-methylidene-*myo*-inositol (18)

To a solution of inositol **12** (1.2 g, 2.18 mmol) in THF (40 ml) under an atmosphere of argon, was added PPh_3 (821 mg, 3.12 mmol, 1.5 eq). The mixture was heated at 50°C. After 8 h the reaction mixture was cooled to RT and H_2O was added (6 ml) while keeping stirring overnight. The mixture was concentrated under reduced pressure and directly used in the next step. The crude extract was dissolved in dry DMF (30 ml) under an atmosphere of argon at 0°C, then triethylamine (507 µl, 3.64 mmol, 2 eq) and dansyl chloride (834 mg, 3.1 mmol, 1.7 eq) were added. The mixture was stirred overnight at RT, after which EA and water were added. The aqueous layer was extracted twice with EA and the combined organic phases were dried ($MgSO_4$), filtered, and concentrated under reduced pressure. The residue was purified by chromatography on silica gel in PE/EA 7/3 to 5/5 to give the product (1.15 g ; 1.76 mmol ; 81%) as a yellow oil. R_f = 0.30 with PE/EA 5/5. ^{1}H NMR (500 MHz, $CDCl_3$) δ 8.51 (d, *J* = 8.5 Hz, 1H, C<u>H</u> (DNS)), 8.30 (d, *J* = 8.6 Hz, 1H, C<u>H</u> (DNS)), 8.18 (dd, *J* = 7.3, 0.9 Hz, 1H, C<u>H</u> (DNS)), 7.53 – 7.43 (m, 2H, C<u>H</u> (DNS)), 7.39 – 7.24 (m, 15H, C<u>H</u> (Bn)), 7.13 (d, *J* = 7.5 Hz, 1H, C<u>H</u> (DNS)), 5.63 (t, $J_{NHHD'}$ = 5.8 Hz, 1H, NH), 5.20 (d, J_{HaHb} = 5.5 Hz, 1H, Ha), 4.81 (d, J_{HbHa} = 5.5 Hz, 1H, Hb), 4.67 (d, *J* = 11.8 Hz, 2H, C<u>H</u>$_2$ (Bn)), 4.63 (s, 2H, C<u>H</u>$_2$ (Bn)), 4.58 (d, *J* = 11.7 Hz, 2H, C<u>H</u>$_2$ (Bn)), 4.28 (s, 2H, H$_1$, H$_3$), 3.92 (d, J_{H4H5} = J_{H6H5} = 6.0 Hz, 2H, H$_4$, H$_6$), 3.86 (s, 1H, H$_2$), 3.69 – 3.59 (m, 2H, H$_{A'}$), 3.53 (t, J_{H5H4} = J_{H5H6} = 6.0 Hz, 1H, H$_5$), 3.38 – 3.35 (m, 2H, H$_{B'}$), 3.34 (t, $J_{HC'HD'}$ = 5.0 Hz, 2H), 3.02 (q, $J_{HD'HC'}$ = 5.4 Hz, 2H, H$_{D'}$), 2.86 (s, 6H, C<u>H</u>$_3$ (DNS)). ^{13}C NMR (126 MHz, $CDCl_3$) δ 151.99 (<u>C</u>, DNS), 137.85 (2<u>C</u>, Bn), 137.81 (<u>C</u>, Bn), 135.42 (<u>C</u>, DNS), 130.35 (<u>C</u>H, DNS), 130.03 (<u>C</u>, DNS), 129.81 (<u>C</u>, DNS), 129.22 (<u>C</u>H, DNS), 128.56, 128.54 (<u>C</u>H, Bn), 128.34 (<u>C</u>H, DNS), 127.99, 127.96, 127.94, 127.91 (<u>C</u>H, Bn), 123.28 (<u>C</u>H, DNS), 119.15 (<u>C</u>H, DNS), 115.28 (<u>C</u>H, DNS), 85.61 (<u>C</u>H$_2$, <u>C</u>HaHb), 82.07 (2<u>C</u>H, C$_4$, C$_6$), 81.31 (<u>C</u>H, C$_5$), 72.12 (2<u>C</u>H, C$_1$, C$_3$), 71.96 (2x<u>C</u>H$_2$, Bn), 71.07 (<u>C</u>H$_2$, Bn), 70.92 (<u>C</u>H$_2$, C$_{A'}$), 70.73 (<u>C</u>H$_2$, C$_{B'}$), 70.29 (<u>C</u>H, C$_2$), 69.29 (<u>C</u>H$_2$, C$_{C'}$), 45.52 (2<u>C</u>H$_3$, DNS), 43.18 (<u>C</u>H$_2$, C$_{D'}$). HRMS *m/z* [M + H]$^+$ calculated for $C_{44}H_{51}N_2O_9S$ 783.3315, found 783.3312.

4.1.2.3. <u>5-*O*-[2-(2-Dansylaminoethoxy)ethyl-*myo*-inositol (16)</u>

A solution of boron trichloride 1M in DCM (5.3 ml, 5.3 mmol, 10 eq) was added to a solution of inositol (**18**) (415 mg, 0.53 mmol) at 0°C. The reaction mixture was stirred for 5 h and MeOH was added to quench the reaction. After evaporation the crude extract was taken into MeOH/Et_2O to form a precipitate which was filtered to give **16** (260 mg, 0.52 mmol; 98%) as a light brown solid.

Mp = 213°C. ^{1}H NMR (500 MHz, MeOD) δ 8.57 (d, *J* = 8.5 Hz, 1H, C*H* (DNS)), 8.36 (d, *J* = 8.7 Hz, 1H, C*H* (DNS)), 8.22 (dd, *J* = 7.3, 1.2 Hz, 1H, C*H* (DNS)), 7.61 (dd, *J* = 8.6, 7.6 Hz, 1H, C*H* (DNS)), 7.59 (dd, *J* = 8.5, 7.3 Hz, 1H, C*H* (DNS)), 7.28 (d, *J* = 7.5 Hz, 1H, C*H* (DNS)), 3.95 (t, $J_{H2H1} = J_{H2H3}$ = 2.8 Hz, 1H, H_2), 3.81 – 3.76 (m, 2H, $H_{A'}$), 3.66 (d, $J_{H4H5} = J_{H6H5}$ = 9.5 Hz, 2H, H_4, H_6), 3.41 – 3.37 (m, 4H, $H_{B'}$, $H_{C'}$), 3.36 (d, $J_{H1H2} = J_{H3H2}$ = 3.0 Hz, 2H, H_1, H_3), 3.07 (t, $J_{HD'HC'}$ = 5.5 Hz, 2H, $H_{D'}$), 2.98 (t, $J_{H5H4} = J_{H5H6}$ =9.3 Hz, 1H, H_5), 2.88 (s, 6H, CH_3 (DNS)). ^{13}C NMR (126 MHz, MeOD) δ 153.17 (*C*, DNS), 137.21 (*C*, DNS), 131.20 (*C*, DNS), 131.16 (*C*H, DNS), 130.94 (*C*, DNS), 130.03 (*C*H, DNS), 129.19 (*C*H, DNS), 124.34 (*C*H, DNS), 120.62 (*C*H, DNS), 116.48 (*C*H, DNS), 85.95 (*C*H, C_5), 73.89 (3*C*H, C_2, C_4, C_6), 73.28 (2*C*H, C_1, C_3), 72.67 (*C*H_2, $C_{A'}$), 71.77 (*C*H_2, $C_{B'}$), 70.59 (*C*H_2, $C_{C'}$), 45.81 (2*C*H_3, DNS), 43.63 (*C*H_2, $C_{D'}$). HRMS *m/z* $[M + Na]^+$ calculated for $C_{22}H_{32}N_2O_9NaS$ 523.1726, found 523.1718.

4.1.2.4. 5-*O*-[2-(2-Dansylaminoethoxy)ethyl-1,2,3,4,6-pentakis-*O*-[bis(benzyloxy)-phosphoryl-*myo*-inositol (21)

To a solution of **16** (80 mg, 0.16 mmol) and 5-phenyltetrazole (257 mg, 1.76 mmol, 11 eq) in dry dichloromethane (8 mL) under argon was added bis(benzyloxy)(*N*,*N*-diisopropylamino)phosphine (290 µL, 0.88 mmol, 5.5 eq). Stirring was continued for 3h30 at room temperature. The reaction mixture was cooled to 0°C and H_2O_2 30% in water (228 µl, 2.23 mmol, 14 éq) was added while stirring. The mixture was allowed to reach room temperature and stirring was continued for 1h at RT. The reaction mixture was diluted with dichloromethane and washed with water and $NaHCO_3$. The aqueous layers were extracted with DCM (3 times) and the organic layers were combined, dried over $MgSO_4$, and concentrated under reduced pressure. The crude extract was washed twice with Et_2O/PE (1/2; 50 ml) and the residue was taken in Et_2O, filtrated and concentrated under reduced pressure to give the product (208 mg ; 1.27 mmol ; 72%) as a yellow oil. R_f = 0.38 with PE/EA 5/5. MW: 1800.48 g.mol^{-1}. ^{1}H NMR (500 MHz, $CDCl_3$) δ 8.51 (d, *J* = 8.7 Hz, 1H, C*H* (DNS)), 8.45 (d, *J* = 8.5 Hz, 1H, C*H* (DNS)), 8.22 (d, *J* = 7.1 Hz, 1H, C*H* (DNS)), 7.44 – 7.34 (m, 2H, C*H* (DNS)), 7.30 – 7.11 (m, 50H, C*H* (Bn)), 7.05 (d, *J* = 7.5 Hz, 1H, C*H* (DNS)), 5.62 (d, $J_{H2H1} = J_{H2H3}$ = 8.9 Hz, 1H, H_2), 5.17 – 4.86 (m, 22H, C*H* (Bn), H_4, H_6), 4.39 (t, $J_{H1H2} = J_{H3H2} = J_{H1H6} = J_{H3H4}$ = 9.5 Hz, 2H, H_1, H_3), 3.83 – 3.72 (m, 2H, $H_{A'}$), 3.41 (t, $J_{H5H4} = J_{H5H6}$ = 9.3 Hz, 1H, H_5), 3.31 – 3.20 (m, 4H, $H_{B'}$, $H_{C'}$), 3.06 (q, $J_{HD'HC'}$ = 5.2 Hz, 2H, $H_{D'}$), 2.81 (s, 6H, CH_3 (DNS)). ^{13}C NMR (126 MHz, $CDCl_3$) δ 151.60 (*C*, DNS), 136.55 (*C*, DNS), 135.97, 135.92, 135.86, 135.82, 135.78, 135.75, 135.73, 135.68 (10*C*, Bn), 129.98 (*C*, DNS), 129.95 (*C*, DNS), 129.76 (*C*H, DNS), 128.67, 128.59, 128.56, 128.53, 128.52, 128.47, 128.45, 128.36, 128.31, 128.28, 128.23, 128.19, 128.13, 128.03, 128.00, 127.96 (50*C*H, Bn, 2*C*H, DNS), 123.23 (*C*H, DNS), 120.01 (*C*H, DNS), 115.14 (*C*H,

DNS), 79.49 (*C*H, C_5), 77.01 (t, *J* = 6.12 Hz, 2*C*H, C_4, C_6), 76.24 (d, *J* = 4.98 Hz, *C*H, C_2), 73.83 (m, 2*C*H, C_1, C_3), 72.76 (*C*H_2, $C_{A'}$), 70.17, 70.13, 70.10, 70.06, 70.01, 69.96, 69.92, 69.86, 69.81, 69.61, 69.57 (12*C*H_2, $C_{B'}$, $C_{C'}$, Bn), 45.50 (2*C*H_3, DNS), 43.23 (*C*H_2, $C_{D'}$). ^{31}P NMR (202 MHz, $CDCl_3$) δ -1.30 (2P), -1.44 (2P), -2.69 (1P). HRMS *m/z* $[M + Na]^+$ calculated for $C_{92}H_{97}N_2O_{24}NaP_5S$ 1823.4738, found 1823.4751.

4.1.2.5. 5-*O*-[2-(2-Dansylaminoethoxy)ethyl-1,2,3,4,6-pentakis-*O*-[bis(benzyloxy)-phosphoryl]-*myo*-inositol (4a)

To a solution of Inositol (**21**) (86 mg, 0.047 mmol) in MeOH (8.6 ml), 10% Pd/C (41 mg) was added and the mixture was stirred under H_2 atmosphere at RT for 2 h. The reaction mixture was filtered over Celite (washed with MeOH and H_2O) and the filtrate was evaporated under reduced pressure. The residue was purified by reverse phase chromatography on C-18 (H_2O as eluent) to give (**4a**) (24 mg, 56%) as a white powder after lyophilization. ^{1}H NMR (500 MHz, D_2O) δ 8.74 (d, *J* = 8.8 Hz, 1H, C*H* (DNS)), 8.44 (d, *J* = 8.6 Hz, 1H, C*H* (DNS)), 8.36 (d, *J* = 7.3 Hz, 1H, C*H* (DNS)), 8.11 (d, *J* = 7.8 Hz, 1H, C*H* (DNS)), 7.90 (q, *J* = 8.4 Hz, 2H, C*H* (DNS)), 4.90 (d, J_{H2H1} = J_{H2H3} = 9.8 Hz, 1H, H_2), 4.37 – 4.23 (m, 4H, H_1, H_3, H_4, H_6), 3.51 (s, 6H, CH_3 (DNS)), 3.39 – 3.33 (m, 3H, $H_{A'}$, H_5), 3.28 (t, $J_{HC'HD'}$ = 4.7 Hz, 2H, $H_{C'}$), 3.23 – 3.18 (m, 2H, $H_{D'}$), 3.12 – 3.07 (m, 2H, $H_{B'}$). ^{13}C NMR (126 MHz, D_2O) δ 138.32 (*C*, DNS), 135.78 (*C*, DNS), 130.48 (*C*H, DNS), 128.63 (*C*, DNS), 128.13 (*C*H, DNS), 127.07 (*C*H, DNS), 126.75 (*C*H, DNS), 125.69 (*C*H, DNS), 125.51 (*C*, DNS), 119.51 (*C*H, DNS), 79.68 (*C*H, C_5), 76.54 (t, *J* = 5.6 Hz, 2*C*H, C_4, C_6), 75.94 (d, *J* = 5.6 Hz, C_2), 73.39 – 72.71 (m, 2*C*H, C_1, C_3), 71.15 (*C*H_2, $C_{A'}$), 69.42 (*C*H_2, $C_{B'}$), 68.51 (*C*H_2, $C_{C'}$), 46.84 (2*C*H_3, DNS), 41.82 (*C*H_2, $C_{D'}$). ^{31}P NMR (202 MHz, D_2O) δ -0.11 (2P), -0.62 (2P), -1.19 (1P). HRMS *m/z* $[M + H]^+$ calculated for $C_{22}H_{38}N_2O_{24}P_5S$ 901.0223, found 901.0216.

4.2. Enzymatic assays

4.2.1. Recombinant enzymes

We worked with recombinant proteins produced by gene overexpression in the yeast *Pichia pastoris*, with methanol as a promotor, following reported procedures [21, 22]. Both enzyme extracts (Phy-A and Phy-C) were produced at the ‘‘Halle de Biotechnologie’’ (UMR IATE, Montpellier, France). The Phy-A enzyme extract was of the same batch as the one described in the literature [11]. It contained 45 mg/mL of total protein mass assayed by the BCA Protein Assay (Pierce), of which 99% is the Phy-A enzyme. The yeast over-expressing the Phy-C enzyme was

obtained following a procedure from the literature [12]. The maximal production of recombinant enzyme (17 mg of total protein, pure at 99%) was obtained after five days of methanol induction. The two enzyme extracts were kept at –20°C before use.

4.2.2. Phytase measurements

We quantified the rate of release of orthophosphate ions (Pi) either from ultrapure sodium phytate (Sigma-Aldrich, Ref P0109) or from dansyl-phytate **4a** to measure the phytase activities with the two substrates. The enzyme assay was carried out as described [11] with some modifications. Briefly, the reaction was carried out in 1.5 mL Eppendorf tubes containing 0.3 mL of 0.025 M acetate buffer pH 5.5, 0.1 mL of 1 mM substrate and 0.1 mL of each diluted enzyme solution (containing 10 and 20 µg of protein.ml^{-1} for PhyA and Phy-C, respectively) or deionized water for control. Calcium was added to the substrate solution (1/3, phytate/calcium) to measure the activity of Phy-C. Two sets of reaction mixtures were prepared to measure the Pi concentrations at time 0 and after 5 min at 25°C. For each time, the reaction was terminated by adding 0.5 mL of tri-chloro-acetic acid (TCA) 10% (w/v). Reaction mixtures were then diluted 21 times with deionized water before measuring Pi concentrations in microplates using the Malachite green method [23] carried out on 200 µL of the diluted solution and 40 µL of each of the two reactants. After 30 min of incubation, absorbance of solutions was measured at 630 nm on a microplate reader. Phytase activity was expressed in µmol.s^{-1}.mg^{-1} of protein.

4.3. Computational details

The 3D structures of Phy-A and Phy-C in complex with the phytate analogue myo-inositol hexakis sulfate were obtained from the Protein Databank (https://www.rcsb.org) under entries 3K4Q and 3AMR, respectively. The structure of the subtrates was drawn and turned into 3D models using Marvin Sketch v20.16 (ChemAxon, http://www.chemaxon.com). Molecular docking was performed with Autodock Vina v1.1.2 [27] using the UCSF Chimera v1.14 [28] interface. The structures corresponding to the poses with the highest docking score were protonated for pH 5.5 using PROPKA 3.0 [29], placed in a TIP3P water shell (8 nm thick) and their energy was minimized within UCSF Chimera with default parameters using the AMBER ff14SB and the AM1-SCC force fields for atomic partial charge calculations in the protein and the ligand, respectively, with the protein backbone constrained to fixed positions. The surface electrostatic potential was calculated with APBS [30]. Molecular graphics were obtained using UCSF ChimeraX v1.1 [31].

Declaration of Competing Interest

The authors declare that they have no known competing financial interests or personal relationships that could have appeared to influence the work reported in this paper.

Acknowledgements

This work was supported by the ANR project "UNLOCKP" (ANR 11 BSV7 015 01; France) awarded to C. P.. C. D. was also supported by the UNLOCKP project through a 12-month post-doctoral fellowship. The authors would like to thank François-Xavier Sauvage (SPO) for his help and advices to produce the recombinant enzymes and Jean-Marc Souquet (Eco&Sols) for his help for phytase activities measurement.

References

1. (a) M.P. Thomas, S.J. Mills, B.V.L. Potter, The "Other" Inositols and Their Phosphates: Synthesis, Biology, and Medicine (with Recent Advances in myo-Inositol Chemistry), Angew. Chemie Int. Ed. 55 (2016) 1614–1650. https://doi.org/https://doi.org/10.1002/anie.201502227. (b) B.V.L. Potter, D. Lampe, Chemistry of Inositol Lipid Mediated Cellular Signaling, Angew. Chemie Int. Ed. English. 34 (1995) 1933–1972. https://doi.org/https://doi.org/10.1002/anie.199519331.
2. (a) F.A. Loewus, P.P.N. Murthy, myo-Inositol metabolism in plants, Plant Sci. 150 (2000) 1–19. https://doi.org/https://doi.org/10.1016/S0168-9452(99)00150-8. (b) C. Cridland, G. Gillaspy, Inositol Pyrophosphate Pathways and Mechanisms: What Can We Learn from Plants?, Mol. . 25 (2020). https://doi.org/10.3390/molecules25122789.
3. (a) J. B. Parys, H. De Smedt, Inositol 1,4,5-trisphosphate and its receptors, Adv. Exp. Med. Biol. 2012, 740 (2012) 255–279, doi: 10.1007/978-94-007-2888-2_11; b) S. B. Shears, S. B. Ganapathi, N. A. Okhale, T. M. H. Schenk, H. Wang, J. D. Weaver, A. Zaremba, Y. Zhou, Defining signal transduction by inositol phosphates, Subcell. Biochem. 59 (2012) 389–412, doi: 10.1007/978-94-007-3015-1_13.
4. H. Sterb, R.F. Irvine, M.J. Berridge, I. Schulz, Release of Ca^{2+} from nonmitochondrial store in pancreatic acinar cells by inositol-1, 4, 5-triphosphate, Nature. 306 (1983) 67–69.
5. B.L. Turner, M.J. Papházy, P.M. Haygarth, I.D. Mckelvie, Inositol phosphates in the environment, Philos. Trans. R. Soc. London. Ser. B Biol. Sci. 357 (2002) 449–469. https://doi.org/10.1098/rstb.2001.0837.
6. (a) C.K. Madsen, H. Brinch-Pedersen, Globoids and Phytase: The Mineral Storage and Release System in Seeds, Int. J. Mol. Sci. 21 (2020) 7519. https://doi.org/10.3390/ijms21207519. (b) J. Wierzbowska, S. Sienkiewicz, M. Zalewska, P. Żarczyński, S. Krzebietke, Phosphorus fractions in soil fertilised with organic waste, Environ. Monit. Assess. 192 (2020) 315, DOI: 10.1007/s10661-020-

8190-9. (c) A.E. Richardson, T.S. George, I. Jakobsen, R.J. Simpson, Plant Utilization of Inositol Phosphates, Inositol Phosphates Link. Agric. Environ. (2007) 242-260.
7. (a) E.J. Mullaney, A.H.J. Ullah, The term phytase comprises several different classes of enzymes, Biochem. Biophys. Res. Commun. 312 (2003) 179–184. https://doi.org/10.1016/j.bbrc.2003.09.176. (b) E.J. Mullaney, A.H.J. Ullah, B. Turner, A. Richardson, E. Mullaney, Phytases: attributes, catalytic mechanisms and applications, Inositol Phosphates Link. Agric. Environ. (2007) 97–110.
8. B. Singh, I. Boukhris, Pragya, V. Kumar, A.N. Yadav, A. FARHAT-KHEMAKHEM, A. KUMAR, D. Singh, M. Blibech, H. Chouayekh, O.A. Alghamadi, Contribution of microbial phytases to the improvement of plant growth and nutrition: A review, Pedosphere. 30 (2020) 295–313. https://doi.org/https://doi.org/10.1016/S1002-0160(20)60010-8.
9. (a) D.F. Berry, D.A. Berry, Tethered phytic acid as a probe for measuring phytase activity, Bioorg. Med. Chem. Lett. 15 (2005) 3157–3161. https://doi.org/10.1016/j.bmcl.2005.04.009. (b) D.F. Berry, C. Shang, L.W. Zelazny, Measurement of phytase activity in soil using a chromophoric tethered phytic acid probe, SOIL Biol. Biochem. 41 (2009) 192–200. https://doi.org/10.1016/j.soilbio.2008.09.011.
10. (a) D.F. Berry, K. Harich, Tetrachlorofluorescein TInsP(5) as a Substrate Analog Probe for Measuring Phytase Activity in Surface Water: Proof of Concept, J. Environ. Qual. 42 (2013) 56–64. https://doi.org/10.2134/jeq2012.0204. (b) Another synthetic phytate has been prepared on a 16 mg scale, to visualize internalization of inositol phosphates by cancer cells, see A.M. Riley, S. Windhorst, H.-Y. Lin, B.V.L. Potter, Cellular Internalisation of an Inositol Phosphate Visualised by Using Fluorescent InsP5, ChemBioChem. 15 (2014) 57–67. https://doi.org/https://doi.org/10.1002/cbic.201300583.
11. C.M. Trouillefou, E. Le Cadre, T. Cacciaguerra, F. Cunin, C. Plassard, E. Belamie, Protected activity of a phytase immobilized in mesoporous silica with benefits to plant phosphorus nutrition, J. SOL-GEL Sci. Technol. 74 (2015) 55–65. https://doi.org/10.1007/s10971-014-3577-0.
12. M. Guerrero-Olazaran, L. Rodriguez-Blanco, J. Gerardo Carreon-Trevino, J.A. Gallegos-Lopez, J.M. Viader-Salvado, Expression of a Bacillus Phytase C Gene in Pichia pastoris and Properties of the Recombinant Enzyme, Appl. Environ. Microbiol. 76 (2010) 5601–5608. https://doi.org/10.1128/AEM.00762-10.
13. N.A. Alcantar, E.S. Aydil, J.N. Israelachvili, Polyethylene glycol–coated biocompatible surfaces, J. Biomed. Mater. Res. 51 (2000) 343–351. https://doi.org/10.1002/1097-4636(20000905)51:3<343::AID-JBM7>3.0.CO;2-D.
14. A.R. Yeager, N.S. Finney, Synthesis of Fluorescently Labeled UDP-GlcNAc Analogues and Their Evaluation as Chitin Synthase Substrates, J. Org. Chem. 70 (2005) 1269–1275. https://doi.org/10.1021/jo0483670.
15. A.J. Oakley, The structure of *Aspergillus niger* phytase PhyA in complex with a phytate mimetic, Biochem. Biophys. Res. Commun. 397 (2010) 745–749. https://doi.org/https://doi.org/10.1016/j.bbrc.2010.06.024.
16. Y.-F. Zeng, T.-P. Ko, H.-L. Lai, Y.-S. Cheng, T.-H. Wu, Y. Ma, C.-C. Chen, C.-S. Yang, K.-J. Cheng, C.-H. Huang, R.-T. Guo, J.-R. Liu, Crystal Structures of *Bacillus* Alkaline Phytase in Complex with Divalent Metal ions and Inositol Hexasulfate, J. Mol. Biol. 409 (2011) 214–224. https://doi.org/https://doi.org/10.1016/j.jmb.2011.03.063.
17. F. Song, J. Zhang, Y. Zhao, W. Chen, L. Li, Z. Xi, Synthesis and antitumor activity of inositol phosphotriester analogues, Org. Biomol. Chem. 10 (2012) 3642–3654. https://doi.org/10.1039/C2OB00031H.
18. X. Yu, S. Eymur, V. Singh, B. Yang, M. Tonga, A. Bheemaraju, G. Cooke, C. Subramani, D. Venkataraman, R.J. Stanley, V.M. Rotello, Flavin as a photo-active

acceptor for efficient energy and charge transfer in a model donor–acceptor system, Phys. Chem. Chem. Phys. 14 (2012) 6749–6754. https://doi.org/10.1039/C2CP40073A.
19. (a) N. T. Rudolf, T. Kaiser, A. H. Guse, G. W. Mayr, C. Schultz, Synthesis and metabolism of the myo-Inositol pentakisphosphates, Liebigs Ann./Recueil, (1987), 1861-1869, https://doi.org/10.1002/jlac.199719970909; (b) N. W. Brown Jr, A. M. Marmelstein, D. Fiedler, Chemical tools for interrogating inositol pyrophosphate structure and function, Chem. Soc. Rev., 45 (2016) 6311, DOI: 10.1039/c6cs00193a ; W. Bannwarth, A. Trzeciak, A simple and effective chemical phosphorylation procedure for biomolecules, Helv. Chim. Acta 70 (1987) 175-186, https://doi.org/10.1002/hlca.19870700122.
20. B.T. Burlingham, T.S. Widlanski, Synthesis and Biological Activity of N-Sulfonylphosphoramidates: Probing the Electrostatic Preferences of Alkaline Phosphatase, J. Org. Chem. 66 (2001) 7561–7567. https://doi.org/10.1021/jo010495q.
21. C. Laborde, P. Chemardin, F. Bigey, Y. Combarnous, G. Moulin, H. Boze, Overexpression of ovine leptin in Pichia pastoris: physiological yeast response to leptin production and characterization of the recombinant hormone, Yeast. 21 (2004) 249–263. https://doi.org/https://doi.org/10.1002/yea.1073.
22. L. Brunel, V. Neugnot, L. Landucci, H. Boze, G. Moulin, F. Bigey, E. Dubreucq, High-level expression of Candida parapsilosis lipase/acyltransferase in *Pichia pastoris*, J. Biotechnol. 111 (2004) 41–50. https://doi.org/https://doi.org/10.1016/j.jbiotec.2004.03.007.
23. T. Ohno, L.M. Zibilske, Determination of Low Concentrations of Phosphorus in Soil Extracts Using Malachite Green, Soil Sci. Soc. Am. J. 55 (1991) 892–895. https://doi.org/https://doi.org/10.2136/sssaj1991.03615995005500030046x.
24. ADF 2020, SCM, Theoretical Chemistry, Vrije Universiteit, Amsterdam, The Netherlands, http://www.scm.com.
25. S. Grimme, S. Ehrlich, L. Goerigk, Effect of the damping function in dispersion corrected density functional theory, J. Comput. Chem. 32 (2011) 1456–1465. https://doi.org/https://doi.org/10.1002/jcc.21759.
26. A. Klamt, G. Schüürmann, COSMO: a new approach to dielectric screening in solvents with explicit expressions for the screening energy and its gradient, J. Chem. Soc. Perkin Trans. 2. (1993) 799–805. doi:10.1039/P29930000799.
27. O. Trott, A.J. Olson, AutoDock Vina: Improving the speed and accuracy of docking with a new scoring function, efficient optimization, and multithreading, J. Comput. Chem. 31 (2010) 455–461. https://doi.org/https://doi.org/10.1002/jcc.21334.
28. E.F. Pettersen, T.D. Goddard, C.C. Huang, G.S. Couch, D.M. Greenblatt, E.C. Meng, T.E. Ferrin, UCSF Chimera—A visualization system for exploratory research and analysis, J. Comput. Chem. 25 (2004) 1605–1612. https://doi.org/https://doi.org/10.1002/jcc.20084.
29. C.R. Søndergaard, M.H.M. Olsson, M. Rostkowski, J.H. Jensen, Improved Treatment of Ligands and Coupling Effects in Empirical Calculation and Rationalization of pKa Values, J. Chem. Theory Comput. 7 (2011) 2284–2295. https://doi.org/10.1021/ct200133y.
30. N.A. Baker, D. Sept, S. Joseph, M.J. Holst, J.A. McCammon, Electrostatics of nanosystems: Application to microtubules and the ribosome, Proc. Natl. Acad. Sci. 98 (2001) 10037–10041. https://doi.org/10.1073/pnas.181342398.
31. E.F. Pettersen, T.D. Goddard, C.C. Huang, E.C. Meng, G.S. Couch, T.I. Croll, J.H. Morris, T.E. Ferrin, UCSF ChimeraX: Structure visualization for researchers, educators, and developers, Protein Sci. 30 (2021) 70–82. https://doi.org/https://doi.org/10.1002/pro.3943.